IET Microwaves, Antennas & Propagation

Research Article

IET Journals
The Institution of Engineering and Technology

A 65% efficient envelope tracking radio-frequency power amplifier for orthogonal frequency division multiplex

ISSN 1751-8725
Received on 14th April 2014
Accepted on 10th November 2014
doi: 10.1049/iet-map.2014.0253
www.ietdl.org

Gavin Tomas Watkins ✉, *Konstantinos Mimis*

Telecommunications Research Laboratory, Toshiba Research Europe Limited, 32 Queen Square, Bristol BS1 4ND, UK
✉ *E-mail: Gavin.watkins@toshiba-trel.com*

Abstract: A high-efficiency radio-frequency (RF) power amplifier (PA) is described for high peak-to-average power ratio (PAPR) orthogonal frequency division multiplexed signals. Envelope tracking is used, where the supply voltage of an RF amplifier is modulated in harmony with the envelope of the RF signal. The envelope modulator is a split-frequency design composed of a switched mode power supply (SMPS) for the low-frequency content, and a hybrid amplifier for the high-frequency part. The hybrid amplifier combines digital switching with a linear amplifier in a transformer coupled push-pull structure. For verification, a 7 dB PAPR 3 MHz bandwidth 3rd generation partnership project long-term evolution (LTE) signal is used. When amplifying the AC component of the LTE envelope signal, 56.2% efficiency is achieved by the hybrid amplifier at 4.6 W output power into a 10 Ω load. Combined with a 94.4% efficient SMPS, the modulator can produce 23.4 W at 83% efficiency. This is combined with an 80.3% efficient 300 MHz RF PA. Together they achieved 65.6% DC-to-RF efficiency at 18.2 W RF output power. The measured PAPR at the amplifier output was 6.5 dB.

1 Introduction

To achieve spectral efficiency at high data rates, contemporary communications and broadcast standards such as 3rd generation partnership project long-term evolution (LTE) [1] and digital video broadcast (DVB) [2] use orthogonal frequency division multiplexing (OFDM) modulation. This comes at the price of a high peak-to-average power ratio (PAPR). Conventional classes A, AB or B power amplifiers (PAs) must be backed-off to accommodate the large amplitude peaks, resulting in low average efficiency.

When a 3 MHz bandwidth LTE signal with quadrature phase shift keying modulation is simulated in advanced wave research's virtual system simulator (VSS), it is found that although these peaks can be 9.8 dB greater than the average signal power, their probability of occurrence is only 0.01%. If these peaks are clipped to 7 dB, an off-the-shelf PA can typically achieve 28% efficiency [3].

Envelope tracking (ET) [4] has shown itself to be an efficient and low-cost method of amplifying high PAPR signals. Since the efficiency enhancement mechanism operates at baseband, a broad operating range [5] and wide radio-frequency (RF) operational bandwidth [6] are possible.

A novel ET architecture is proposed in this paper based around a highly efficient hybrid linear amplifier combining both analogue and digital sections capable of state-of-the-art efficiency. An overview of the ET architecture is given in Section 2. The design with regard to contemporary OFDM signals, detailed operation and implementation of the hybrid amplifier is described in Section 3. Section 4 reports the results of the hybrid amplifier and complete system, and benchmarks this paper against comparable systems published in the literature. Section 5 concludes this paper.

2 Envelope tracking

The ET principle involves manipulating the supply voltage to an RF PA in harmony with the instantaneous envelope amplitude of the transmitted signal. This ensures that the amplifier always remains in an efficient region of its transfer characteristic, that is, close to compression. For this reason, class E PAs are well suited to this [7] or other amplifiers operating in their saturation region such as class AB [8] or class F [9].

The optimum envelope modulator is a high-frequency switched mode power supply (SMPS) or class S amplifier. In practice, efficiency drops sharply at high switching frequencies because of capacitive losses [10]. A more practical approach is the split-frequency architecture shown in Fig. 1 where the envelope signal is split into high- and low-frequency components [11]. It is found by analysing the LTE envelope signal in the frequency domain that ~80% of the envelope power resides at DC [11], equivalent to the average value of the signal. An efficient solution is therefore possible if the low-frequency component is amplified by an SMPS and the high frequency by a linear class B amplifier [12]. Efficiency can be further enhanced if the linear amplifier is a class G type [7].

The efficiency of a split-frequency envelope modulator (η_{MOD}) is a factor of SMPS efficiency (η_{SMPS}), the linear amplifier's efficiency (η_{AMP}) and the proportion (α) of the envelope signal amplified by the SMPS

$$\eta_{MOD} = \frac{1}{\alpha/\eta_{SMPS} + 1 - \alpha/\eta_{AMP}} \quad (1)$$

with up to 97% SMPS efficiency possible [13], the biggest factor impacting modulator efficiency is the linear amplifier.

3 Hybrid linear amplifier

A typical class B amplifier can achieve 31% efficiency when amplifying the high-frequency component of an LTE signal [12] and 39% when two level class *G* is used [7]. Although efficiency can be enhanced by increasing the number of class *G* levels, extra power supplies are needed. An alternative approach proposed here is a hybrid push-pull technique combining digital switching with a linear analogue amplifier. Hybrid modulators have previously been proposed, but only in single-ended designs [14].

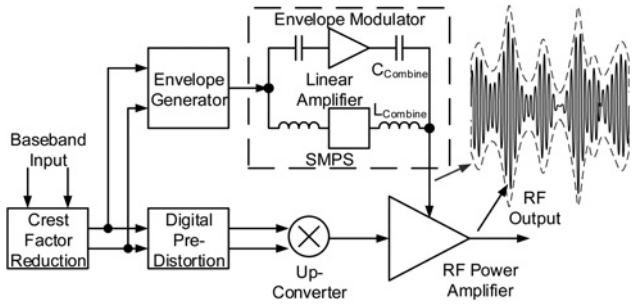

Fig. 1 *Split-frequency modulator ET RF PA. 208 × 101 mm (72 × 72 dots per inch (DPI))*

The hybrid technique works by effectively reducing the voltage dropped across the linear amplifier, in a similar manner to the class G architecture. Linear amplifiers are generally inefficient when amplifying high dynamic range signals, but stepping the supply voltage between a number of discrete levels in harmony with the envelope signal can increase efficiency as shown in Fig. 2 for the case of a split-frequency envelope modulator.

The original envelope signal is shown in Fig. 2*a*. The high-frequency component shown in Fig. 2*b* has asymmetric positive and negative excursions. For a 7 dB PAPR signal, the positive to negative excursions have a 3:2 ratio.

The high-frequency component is compared with a set of equally spaced thresholds which control the linear amplifier supply voltage as shown in Fig. 2*c*. Hence the voltage drop across the linear amplifier is reduced as shown in Fig. 2*d*. It can be seen that the area between the envelope signal and supply voltage in Fig. 2*d* is significantly less than that of Fig. 2*b*. This area is equivalent to the power dissipation of the linear amplifier.

The theoretical efficiency of the hybrid amplifier is a factor of the signal PAPR and the number of voltage levels. For ET where the envelope voltage tracks the transmitted signal, the PAPR is the ratio of the peak voltage envelope voltage (V_{PEAK}) to its RMS value (V_{RMS})

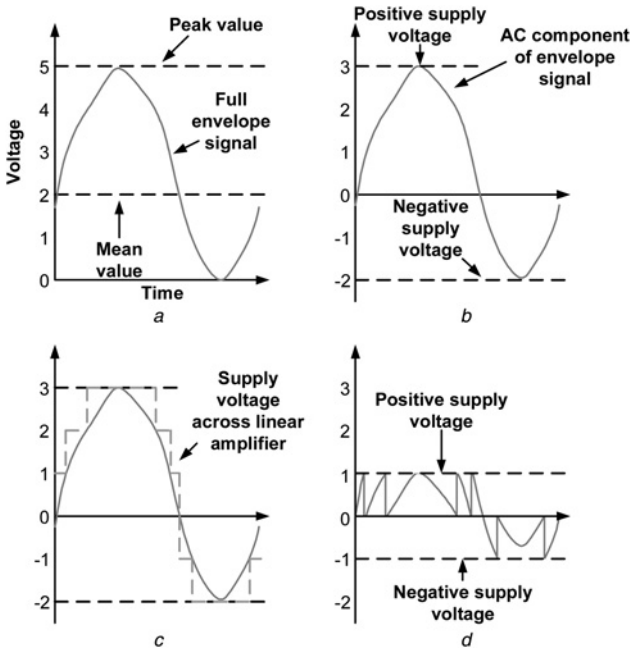

Fig. 2 *Operation of a hybrid split-frequency modulator*

a Original envelope signal
b High-frequency component
c Supply voltage across to the linear amplifier switched in discrete steps so as to reduce the voltage drop *d* Voltage drop. 196 × 213 mm (72 × 72 DPI)

Table 1 Simulated modulator efficiency

N	N_{POS}	N_{NEG}	PAPR, dB	Linear amplifier efficiency, %	Modulator efficiency, %
3	2	1	8.5	39.4	74.1
3	2	1	9.8	33.2	69.2
5	3	2	7	59.6	84.9
5	3	2	9.8	46.5	78.6
6	4	2	8.6	59.3	84.8
6	4	2	9.8	54	82.5
7	4	3	6.4	69.8	88.6
7	4	3	9.8	54	82.5
8	5	3	7.6	69.4	88.5
8	5	3	9.8	60.1	85.1

$$\mathrm{PAPR} = 20 \cdot \mathrm{Log}\left(\frac{V_{PEAK}}{V_{RMS}}\right) \tag{2}$$

with 80% of the envelope signals power near to DC, the mean envelope voltage (V_{MEAN}) accounts for 89% of V_{RMS}

$$\mathrm{PAPR} = 20 \cdot \mathrm{Log}\left(\frac{0.89 \cdot V_{PEAK}}{V_{MEAN}}\right) \tag{3}$$

For maximum efficiency, the total number of switching levels (N, where $N = 5$ in Fig. 2) should be optimised for a given PAPR

$$\mathrm{PAPR} = 20 \cdot \mathrm{Log}\left(\frac{0.89 \cdot (N_{NEG} + N_{POS})}{N_{NEG}}\right) \tag{4}$$

$$V_{MEAN} = N_{NEG} \tag{5}$$

$$V_{PEAK} = N_{NEG} + N_{POS} \tag{6}$$

where N_{POS} is the number of positive levels of the high-frequency component and N_{NEG} is the number of negative levels.

Using (4) the optimum PAPR for a given N is shown in Table 1. The linear amplifier and total modulator efficiencies are determined by simulating the modulator with the LTE envelope signal and assuming a 95% efficient SMPS. Also shown in Table 1 are the results if the PAPR is not optimised for a given N, but left at 9.8 dB. These results are bandwidth independent.

Table 1 verifies that a high modulator efficiency is possible with the hybrid amplifier even when the PAPR is not optimised for N. Generally efficiency drops as PAPR increases, but this is not necessarily the case for a hybrid amplifier where efficiency increases with N because of reduced voltage drop across the linear amplifier. Table 1 shows a trade-off between N, efficiency and PAPR. For this paper, $N = 5$ was chosen to illustrate the principle. It is a fair compromise between complexity, PAPR and efficiency. This is compared with both a class B amplifier and the standard

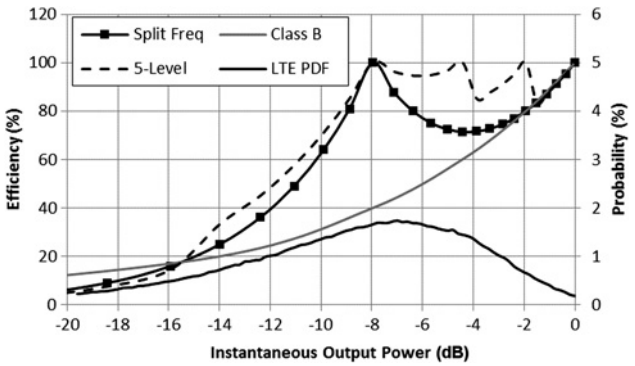

Fig. 3 *Theoretical modulator efficiencies against normalised instantaneous output power, and the PDF of the 7 dB PAPR 3 MHz LTE signal. 264 × 158 mm (72 × 72 DPI)*

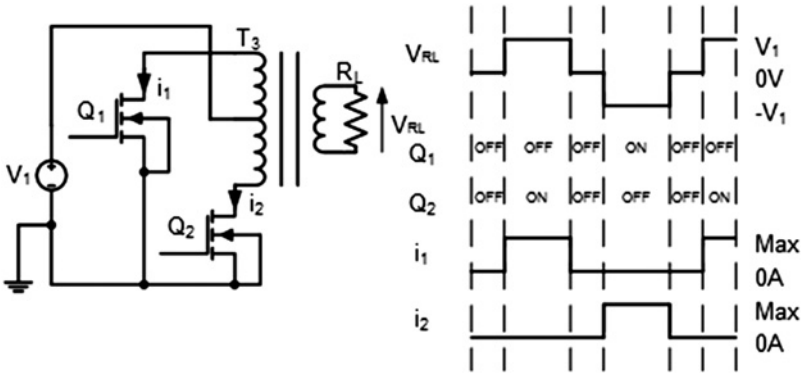

Fig. 4 *Push-pull transformer coupled converter. 164 × 73 mm (72 × 72 DPI)*

split-frequency modulator in Fig. 3. Also included in Fig. 3 is the probability distribution function (PDF) of the LTE envelope signal.

The basic split-frequency modulator has two efficiency peaks, assuming ideal components, that is, a 100% efficient SMPS and zero quiescent current consumption. The equally spaced five-level hybrid amplifier has four efficiency peaks as the voltage drop across the linear amplifier approaches zero. There is also a small increase in efficiency at −14 dB during the negative supply voltage switching.

3.1 Push-pull hybrid amplifier

To both sink and source currents, a push-pull hybrid amplifier is required. High-speed complementary pairs of bipolar or metal–oxide field effect transistors (MOSFETs) are not readily available, so a transformer coupled push-pull configuration [15] is adopted. A switching transformer coupled push-pull stage is shown in Fig. 4 where the ends of the transformer are alternatively switched to the negative supply rail by *N*-channel MOSFETs to recreate an AC output voltage.

Three unique voltage states are produced across R_L (V_{RL}): V_1, 0 V and $-V_1$. To produce a linear output, the centre tap of the transformer can be driven by a single-ended linear amplifier or high bandwidth SMPS [16].

Additional MOSFETs can be included connected to different potentials to increase N_{POS} and N_{NEG}. To create the additional positive voltage state, a charge pump [17] can raise the switching voltage above the supply. Combining a split rail power supply with charge pump and a linear amplifier produces the hybrid architecture shown in Fig. 5, where Q_6 and Q_7 are responsible for N_{NEG}; and Q_3, Q_4 and Q_5 for N_{POS}. Q_3 and Q_4 form a switch which drives charge pump capacitor C_1, so that its negative terminal is either at $-V_1$ or $2\times -V_1$. Q_3–Q_7 are switched in harmony with the instantaneous envelope amplitude as indicated in Fig. 2. The operation of the charge pump switching cell-based around Q_3, Q_4 and Q_5 is explained further in Fig. 6, where R_L takes the place of half of T_2.

Fig. 6 shows the current flow of the four states in grey. In Fig. 6*a*, Q_4 and Q_5 are open so no current flows through R_L, and therefore 0 V appears across it. Current is however permitted to flow into C_1 through Q_3, allowing it to charge to a potential of $V_1 + V_2$ or two times V_1. Closing Q_4 and opening Q_3 as shown in Fig. 6*b* results in V_1 appearing across R_L as current flows to ground through Q_4. In Fig. 6*c*, Q_5 is closed while Q_3 and Q_4 are open. Current flows through Q_5 so $2\times V_1$ appears across R_L. In Fig. 6*d*, Q_4 and Q_5 are closed so that C_1 is in series with V_1 resulting in three times V_1 produced across R_L.

3.2 Implementation

A hybrid amplifier based on Fig. 5 was implemented on FR4 and is shown in Fig. 7. It will be noted in Fig. 7 that the efficiencies of both the hybrid amplifier and the SMPS are high enough that heat sinks are not needed.

With a supply voltage of ±15 V, the maximum theoretical peak-to-peak output voltage of the hybrid amplifier is 75 V corresponding to a positive excursion of 45 V and a negative of 30 V. With an expected PA drain impedance of 10 Ω, this was reduced to 37.5 V peak-to-peak with a 2:2:1 ratio transformer. The

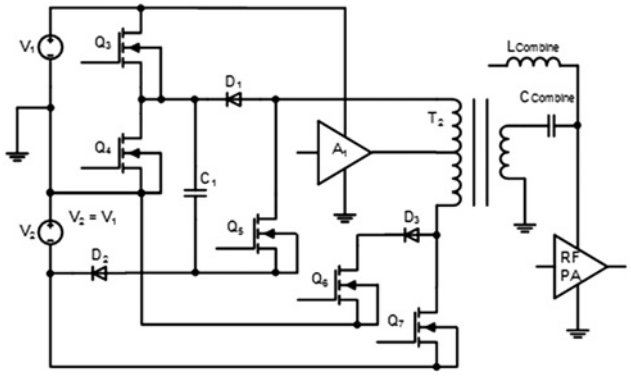

Fig. 5 *Simplified multi-level push-pull hybrid amplifier. 156 × 92 mm (72 × 72 DPI)*

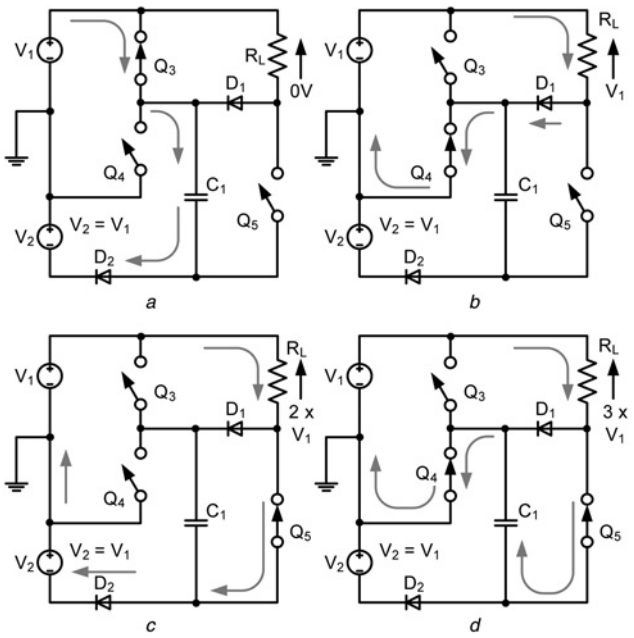

Fig. 6 *Operation of charge pump switching cell, current path shown in grey. 159 × 161 mm (72 × 72 DPI)*

IET Microw. Antennas Propag., 2015, Vol. 9, Iss. 7, pp. 676–681

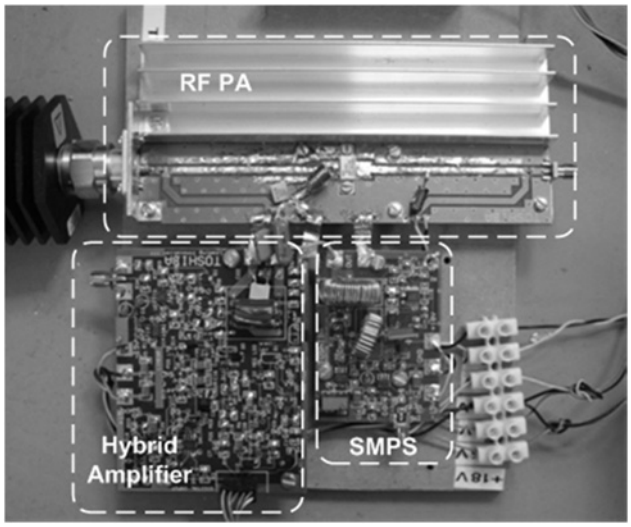

Fig. 7 *Photograph of ET RF PA. 144 × 120 mm (72 × 72 DPI)*

transformer must operate from the cross-over frequency of the paths (~16 kHz) to greater than the channel bandwidth [11], and have a low insertion loss. To produce a 2:2:1 ratio, five lengths of 27 AWG enamelled copper wire were twisted together in a bifilar fashion and wound on a ferrite core (Fair-Rite part number 2643375002). Four of the windings were connected in series for the centre tapped primary, with the remaining winding forming the secondary. The 3 dB bandwidth extended from below 1 kHz to 14 MHz.

The switching transistors Q_3–Q_5 in Fig. 5 are ZVN2110As. Q_5 requires an isolated level shifter since its source switches between −15 and −30 V. A linear differential amplifier fulfils this role while providing sufficient peak-to-peak output swing and bandwidth. The linear amplifier uses two parallel PD85004 RF laterally diffused metal oxide semiconductor (LDMOS) transistors in the feedback path of an operational amplifier similar to that shown in [12]. Two transistors are required to withstand the peak current. The SMPS for the low-frequency path of the modulator was developed around a Texas Instruments LM25088, which has previously been shown to be suitable for split-frequency modulators [12]. A simplified schematic of the SMPS is shown in Fig. 8.

A filtered version of the envelope signal is introduced into the feedback path of the SMPS. Feedback comes via block β which sets the overall gain and output voltage. Classically, SMPSs have a low bandwidth because of their large output smoothing capacitor (C_F) – often in the order of hundreds or even thousands of microfarads. In this implementation C_F is 1 µF, resulting in a bandwidth of 18 kHz. A +18 V supply was required to accommodate the peak excursions of the low-frequency component.

3.3 Radio-frequency PA

To verify the system performance a suitable RF PA was developed. A class E inspired PA was produced around an NXP BLF871

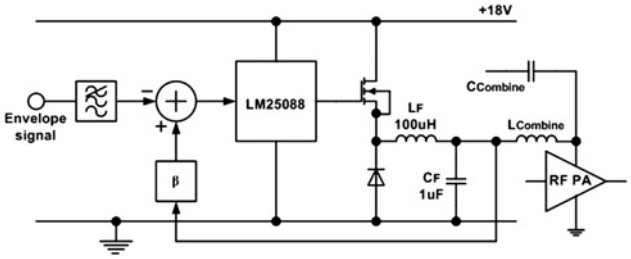

Fig. 8 *Simplified schematic of SMPS. 207 × 84 mm (72 × 72 DPI)*

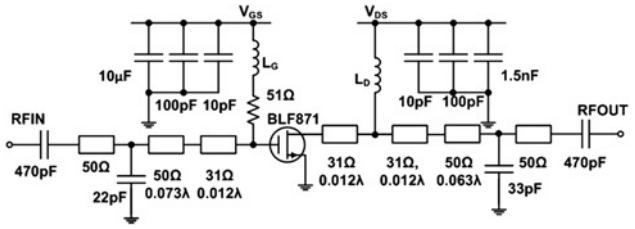

Fig. 9 *Schematic of PA. 238 × 85 mm (72 × 72 DPI)*

LDMOS device [3]. Although the BLF871 has a large output capacitance (C_{OUT}) of 30 pF, efficient class E operation is still possible at very high frequency (30–300 MHz). The estimated maximum operating frequency (F_{MAX}) of a class E amplifier is [18]

$$F_{MAX} = \frac{P_{OUT}}{2 \cdot \pi^2 \cdot C_{OUT} \cdot V_{DS}^2} \tag{7}$$

P_{OUT} is the output RF output power, V_{DS} is the drain source voltage and C_{OUT} is the capacitance at the drain terminal including device and package stray parasitic components. Equation (7) predicts an F_{MAX} or 137 MHz for the BLF871 in this application, although this assumes that the output network presented to the transistor has a high Q, which is unlikely for a realistic PA. Practically, 300 MHz was chosen as a compromise between efficiency and bandwidth, so as to accommodate the 3 MHz LTE signal. Although there are no bands using wideband OFDM type signals (i.e. LTE and DVB) at 300 MHz, this PA is for illustrative purposes only. A gallium nitride transistor with a lower C_{OUT} than the BLF871 could push the operating frequency up to the more usual LTE bands about 800 MHz.

A transmission line architecture is used, whereby matching networks are composed of series inductors formed from lengths of transmission lines with discrete shunt capacitors. A schematic of the PA is shown in Fig. 9, where V_{GS}, the gate voltage, was adjusted for a quiescent current consumption of 450 mA (10% of I_{DSmax}) to set a comfortable class AB bias.

By simulating the output network, the fundamental load impedance was found to be 4.7 + 10.3j Ω with a Q of 3. Such a low Q will tend to detune (7) away from the classic class E operating conditions. The imaginary component of the load impedance suggests class E operation for the PA, but the large load angle and high quiescent current result in non-classical class E. The PA was tuned for highest efficiency at the back-off region. Owing to the low operating frequency, the effects of parasitic inductance and capacitance of the transistor are small. The second harmonic (600 MHz) impedance was 5.2 + 73j Ω and the third (900 MHz) 13.5 + 225j Ω. The high impedances presented at the harmonic zones ensure that little power is dissipated there, hence maintaining a high efficiency.

4 Results

Two LeCroy ArbStudio arbitrary signal generators were used to drive the complete ET PA giving a total of five channels that were split between analogue and digital outputs. The hybrid amplifier required one analogue, and one digital for switching MOSFETs Q_3–Q_7. The SMPS requires one analogue channel. Two more analogue channels are needed to generate the I and Q signals to modulate a HP8780A RF vector signal generator.

The linear amplifier had a measured small signal bandwidth of 8 MHz. Although less than the recommended five times the signal bandwidth, it is sufficient for a 3 MHz bandwidth signal with some degradation in the adjacent channel power ratio (ACPR) [19]. The measured rise time was 40 ns and fall time was 35 ns when excited with a square wave. The output signal amplitude was 14 V peak-to-peak; indicating a slew rate of at least 350 V/µs.

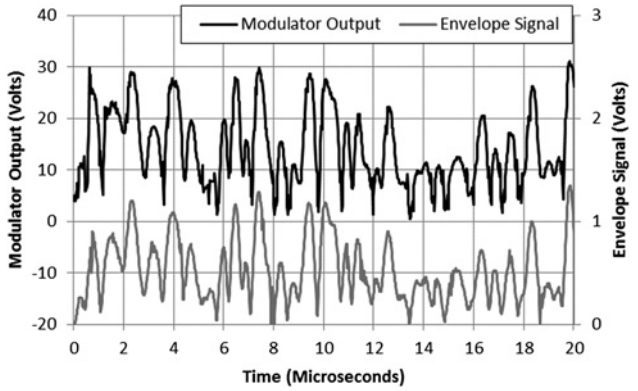

Fig. 10 *Time-domain waveforms of modulator. 264 × 158 mm (72 × 72 DPI)*

Under target operating conditions, the hybrid amplifier reproduced the AC component of the 7 dB 3 MHz LTE envelope signal at 4.62 W into the 10 Ω load. Power consumption was 8.22 W, resulting in an efficiency of 56.2%, close to the expected 59.6% shown in Table 1 for an $N = 5$ architecture. The peak positive excursion was 18.6 V and the negative excursion was −13.2 V.

When the hybrid amplifier and SMPS were combined, an envelope output power of 23.4 W was produced into the 10 Ω load. DC power consumption was 28.2 W resulting in an efficiency of 83%. The modulator input and output waveforms are shown in Fig. 10, and the transfer response of the complete modulator in Fig. 11. The spreading of the points in Fig. 11 is because of switching glitches in the hybrid amplifier. The individual glitches are visible in Fig. 10. These glitches are caused by the timing misalignment between the switching stages. Resistor–capacitor–diode delay networks were added to prevent the switching states overlapping [15], but not optimised in these results. At an output voltage of 13.5 V, the SMPS exhibited an efficiency of 95%.

The peak output voltage was 32.2 V, equivalent to 6.5 dB PAPR. With an AC component of 6.6 V_{rms}, equivalent to 4.36 W α in (1) was determined as 0.81. The SMPS efficiency was therefore

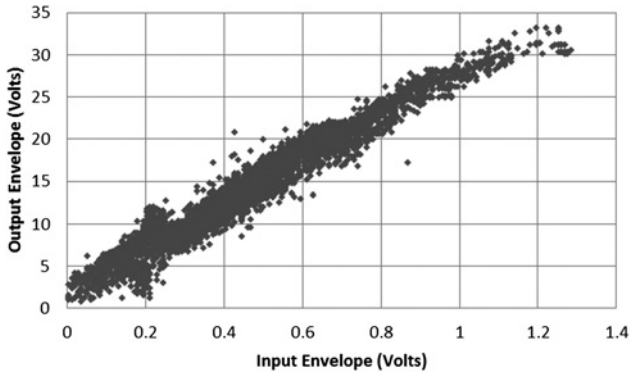

Fig. 11 *Transfer response of complete modulator. 264 × 159 mm (72 × 72 DPI)*

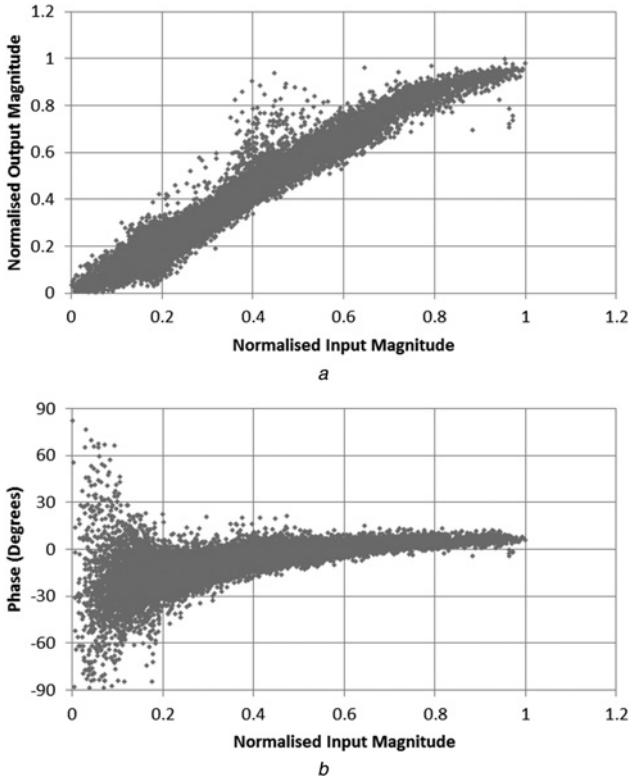

Fig. 12 *Dynamic and averaged*

a AM–AM

b AM–PM response of the complete system. 264 × 317 mm (72 × 72 DPI)

94.4%, and the hybrid amplifier 54.2%. The normalised root-mean-square error (NRMSE) [20] of the complete envelope modulator was −26.7 dB with reference to the signal generated in VSS after crest factor reduction was applied.

4.1 Complete system

Tuning the PA for maximum efficiency resulted in 80.3% at 17.6 W output power (P_{OUT}) at a V_{DS} of 15.3 V, equivalent to the RMS output voltage of the modulator. The drain impedance of the PA under these conditions was 10.7 Ω.

After time aligning of the RF carrier and envelope signal [21], an efficiency of 65.6% at 42.59 dBm (18.16 W) P_{OUT} was achieved with the 3 MHz LTE signal. The output PAPR was 6.5 dB, matching that of the modulator. The first channel ACPR was −27.7 dBc for the lower and −27.1 dBc for the upper. The ACPR degradation is largely because of the switching noise as indicated by the AM–AM and AM–PM dynamic responses shown in Fig. 12. Further optimisation of the timing alignment could reduce the modulator noise and improve the ACPR.

Comparing Figs. 11 to 12, there is a small increase in the spreading of the points when the RF PA is introduced. This suggests a frequency dependent interaction between modulator and PA hinting at memory effects. However, the effect is small compared with the spreading introduced by timing misalignment which is the major factor to degrade the ACPR. The primary target of this paper although was

Table 2 Comparison of state-of-the-art ET amplifiers for LTE

References	Signal bandwidth, MHz	RF frequency, MHz	P_{OUT}, W	DC-to-RF efficiency, %	PAPR, dB
[22]	10	850	80	51.2	7.5
[23]	10	870	70.8	58.5	6.5
[24]	10	780	22.8	59.9	7.5
[8]	5	889	10.3	60.2	6.5
this work	3	300	18.2	65.6	6.5

IET Microw. Antennas Propag., 2015, Vol. 9, Iss. 7, pp. 676–681

to produce a high-efficiency modulator. Improvements to linearity will be dealt with separately. From the AM–AM and AM–PM measurements, the error vector magnitude (EVM) was estimated as 24%. This is not a true EVM measurement although, since the LTE signal cannot be demodulated back down to the raw baseband data at this time for comparison.

Compared with other published results, this paper achieves the highest efficiency for an LTE amplifier of its class based on P_{OUT} and PAPR as shown in Table 2. It should be noted that the other amplifiers in Table 2 use Gallium Nitride RF devices, whereas this paper uses LDMOS, which accounts for their higher operating frequency. Although the signal bandwidth is also less than the other published results, this could be increased with better switching circuitry and more accurate timing alignment.

5 Conclusions

Contemporary OFDM-based modulation schemes such as LTE and DVB have high PAPRs, meaning that conventional linear RF PAs operate at a low efficiency if the full signal peaks are to be reproduced. ET is a low cost and practical way of increasing the efficiency of an RF PA when subjected to such signals.

In a split-frequency envelope modulator, the linear amplifier has the largest impact on overall system performance, particularly efficiency. To improve efficiency, a hybrid technique is proposed whereby the supply voltage to a linear amplifier is digitally switched between a range of potentials to reduce the voltage drop across it and hence losses. A prototype was produced with three potentials for the positive excursions and two for the negative. The additional positive potential was produced with a capacitive charge pump. This is designed to accommodate the AC component of a 7 dB PAPR 3 MHz LTE envelope signal.

A system based on a transformer coupled push-pull amplifier using only *N*-channel MOSFETs was developed. Practically 56.2% efficiency was achieved for the hybrid amplifier. Combined with an appropriate SMPS, measured efficiency was 83% at 23.4 W envelope power. The NRMSE for the modulator was −26.7 dB.

To evaluate the full system an RF amplifier achieving 80.3% efficiency and 17.6 W output power at a V_{DS} of 15.3 V was designed. Combined, a total DC-to-RF efficiency of 65.6% was possible at 18.2 W P_{OUT}. Operating frequency was 300 MHz. The PAPR at the output was measured as 6.5 dB, and the ACPR −27.4 dBc. From the AM–AM and AM–PM results the EVM was estimated as 24%.

6 Acknowledgments

The authors thank all at the Toshiba Research Europe Limited for their support in this work and also Keiichi Yamaguchi from the Toshiba's Research and Development Centre in Tokyo for his helpful advice.

7 References

1 TS 36.211 E-UTRA specifications
2 The DVB Project ETSI EN 302 755 specifications
3 BLF6G15 L-500H and BLF871 datasheets available from NXP
4 Kahn, L.R.: 'Single sideband transmission by envelope elimination and restoration', *Proc. Inst. Radio Eng.*, 1952, **40**, pp. 803–806
5 Bacque, L., Bouysse, P., Rebernak, W., *et al.*: 'High-current-high-speed dynamic bias control system applied to a 100 W wideband push-pull amplifier', *IEEE Trans. Microw. Theory Tech.*, 2008, **56**, (12), pp. 2798–2805
6 Kim, D., Kang, D., Kim, J., Cho, Y., Kim, B.: 'Wideband envelope tracking power amplifier for LTE applications'. 2012 IEEE Radio Frequency Integrated Circuit Symp., June 2012, pp. 275–276
7 Watkins, G., Zhou, J., Morris, K.: '>41% efficient 10 W envelope modulated LTE downlink power amplifier'. 2011 41st European Microwave Conf., 10–11 October 2011, pp. 260–263
8 Kim, J., Son, J., Jee, S., Kim, S., Kim, B.: 'Optimization of envelope tracking power amplifier for base-station applications', *IEEE Trans. Microw. Theory Tech.*, 2013, **61**, (4), pp. 1620–1627
9 Kim, J.H., Son, H.S., Kim, W.Y., Park, C.S.: 'Envelope amplifier with multiple-linear regulator for envelope tracking power amplifier', *IEEE Trans. Microw. Theory Tech.*, 2013, **61**, (11), pp. 3951–3960
10 Strydom, J.: 'eGan FETs for envelope tracking'. Efficiency Power Converters (EPC) White Paper: WP013
11 Raab, F.H.: 'Split-band modulator for Kahn-technique transmitters'. 2004 IEEE MTT-S Int. Microwave Symp. Digest, June 2004, vol. 2, pp. 887–890
12 Watkins, G.T.: 'High bandwidth class B totem pole power amplifier for envelope modulators', *IET Electron. Lett.*, 2013, **49**, (2), pp. 127–129
13 Balasubramaniam, R., Contenti, C.: 'Industrial grade 25 A versatile voltage regulator', *Power Electron. Eur.*, 2013, (3), pp. 41–43
14 Vasic, M., Garcia, O., Loiver, J.A., Alou, P., Diaz, D., Cobos, J.A.: 'Multilevel power supply for high efficiency RF amplifiers', *IEEE Trans. Power Electron.*, 2009, **25**, (4), pp. 1233–1238
15 Pressman, A.I., Billings, K., Morey, T.: 'Switching power supply design' (McGraw-Hill, 2009, 3rd edn.), ISBN 978-0-07-148272-1, Chapter 2, pp. 45–75
16 Williams, J.: 'Step-down switching regulators'. Linear Technology Application Note 35, August 1989, pp. 14–16
17 Horowotz, P., Hill, W.: 'The art of electronics' (Cambridge University Press, 1987), ISBN 0521 23151 5, p. 39
18 Thian, M., Fusco, V.F.: 'Transmission-line class-E power amplifier with extended maximum operating frequency', *IEEE Trans. Circuits Syst. II, Express Briefs*, 2011, **58**, (4), pp. 195–198
19 Rabb, F.H.: 'Intermodulation distortion in Kahn-technique transmitters', *IEEE Trans. Microw. Theory Tech.*, 1996, **44**, (12), pp. 2273–2278
20 Hong, Y., Mukai, K., Gheidi, H., Shinjo, S., Asbeck, P.M.: 'High efficiency GaN switching converter IC with bootstrap driver for envelope tracking applications'. IEEE Radio Frequency Integrated Circuits Symp., June 2013, pp. 353–356
21 Wang, F., Kimball, D.F., Popp, J.D., *et al.*: 'An improved power-added efficiency 19 dBm hybrid envelope elimination and restoration power amplifier for 802.11 g WLAN applications', *IEEE Trans. Microw. Theory Tech.*, 2006, **54**, (12), pp. 4086–4099
22 Giovannelli, N., Cidronali, A., Mercanti, M., Hernaman, R., Wimpenny, G., Manes, G.: 'A 80 W broadband GaN HEMT envelope tracking PA harmonically tuned for WCDMA and LTE with 50% average efficiency'. 2012 IEEE MTT-S Microwave Symp. Digest (MTT), June 2012, pp. 1–3
23 Cidronali, A., Giovannelli, N., Vlasits, T., Hernaman, R., Manes, G.: 'A 240 W dual-band 870 and 2140 MHz envelope tracking GaN PA designed by a probability distribution conscious approach'. 2011 IEEE MTT-S Int. Microwave Symp. Digest (MTT), June 2011, pp. 1–4
24 Yan, J.J., Theilmann, P., Kimball, D.F.: 'A high efficiency 780 MHz GaN envelope tracking power amplifier'. 2012 IEEE Compound Semiconductor Integrated Circuit Symp. (CSICS), October 2012, pp. 1–4